16th ICAAR LISBOA 2020-2022

16th International Conference on
Alkali-Aggregate Reaction in Concrete
Lisboa | LNEC | Portugal | 31 May - 2 June 2022

http://icaar2020-2022.lnec.pt

Quantification of the extent of alkali-silica reaction occurring in cemented waste packages based on simplified model systems

Nicolas Courtois [(1)], Céline Cau Dit Coumes [(2)], Philippe Gaveau [(3)], Arnaud Poulesquen [(4)], Jérémy Haas [(5)], Seif Ben Hadj Hassine [(6)], David Bulteel [(7)]

(1) CEA, DES, ISEC, DE2D, SEAD, LCBC, Marcoule, France, nicolas.courtois@cea.fr

Univ. Lille, Institut Mines-Télécom, Univ. Artois, Junia, ULR 4515 - LGCgE, Lille, France

IMT Lille Douai, Institut Mines-Télécom, Centre for Materials and Processes, Lille, France

(2) CEA, DES, ISEC, DE2D, SEAD, LCBC, Marcoule, France, celine.cau-dit-coumes@cea.fr

(3) ICGM, UMR 5253, CNRS UM ENSCM, Montpellier, France, philippe.gaveau@umontpellier.fr

(4) CEA, DES, ISEC, DE2D, SEAD, LCBC, Marcoule, France, arnaud.poulesquen@cea.fr

(5) CEA, DES, ISEC, DE2D, SEAD, LCBC, Marcoule, France, jeremy.haas@cea.fr

(6) ONDRAF/NIRAS, Brussels, Belgium, s.benhadjhassine@nirond.be

(7) Univ. Lille, Institut Mines-Télécom, Univ. Artois, Junia, ULR 4515 - LGCgE, Lille, France

IMT Lille Douai, Institut Mines-Télécom, Centre for Materials and Processes, Lille, France, david.bulteel@imt-lille-douai.fr

Abstract

Nuclear power production generates radioactive waste, the management of which is an important industrial and environmental issue. Low – or intermediate – level radioactive aqueous waste can be concentrated by evaporation, stabilized and solidified with Portland cement before being sent to disposal. Interactions can however occur between the waste and the cement phases or aggregates, and decrease the stability of the final waste forms.

The formation of a gel-like product, which results from an alkali-aggregate reaction, has been recently observed at the surface of cemented drums of evaporator concentrates. Its properties differ however from those usually reported for alkali-silica gels: (i) very low calcium concentration, (ii) significant presence of Zn^{2+}, Cl^-, $B(OH)_4^-$ and SO_4^{2-} ions, (iii) high formation rate, (iv) rather limited damage of the cementitious matrix considering the amount of gel produced. This work investigates the progress of alkali-silica reaction in the cemented drums at early age, by studying the deterioration rate of the aggregates in model systems.

A synthetic alkaline solution, which mimics the pore solution including the waste, was used to degrade the siliceous aggregates under controlled conditions. Determination of the extent of degradation caused by alkali-silica reaction was achieved by weighing the residual flint aggregates and by quantifying their deterioration state by ^{29}Si NMR, BET and gas pycnometry.

Keywords: *alkali-silica reaction; extent of reaction; flint aggregate; model system; nuclear waste immobilization.*

1. INTRODUCTION

Nuclear power production generates radioactive wastes, the management of which is an important industrial and environmental issue. Thus, low - or intermediate - level radioactive aqueous waste streams can be concentrated by evaporation, stabilized and immobilized with a hydraulic binder, usually a Portland cement or a blast furnace slag cement, before being sent to disposal. Interactions can however occur between some waste components and the cement phases or aggregates, and decrease the stability of the final waste forms. Aqueous waste streams, produced by Doel nuclear power plant in Belgium, were concentrated by evaporation, leading to evaporator concentrates with a high number of chemical species. The presence of boron and the acidic pH of the waste led to the addition of sodium hydroxide in order to maintain the workability of the fresh concrete and avoid a too long setting time. The concentrate was then stored in tanks at 80°C to avoid borate crystallization, until the cementation step. This latter consisted in an in-drum mixing process, in which the raw materials were introduced in the order detailed hereinafter. Firstly, aggregates were introduced into the empty drum. Afterwards, the

warm concentrate was incorporated. Lastly, the cement was added to the mixture. The warm concentrate incorporation led to a peculiar thermal history of the drums, with a temperature rise up to 90°C, as shown in Figure 1.1.

The formation of a gel-like product was observed in 2013, at the surface of some of the waste packages cemented between 1983 and 2012, leading in some cases to cracks in the stabilization matrix and to the leaking of some canisters [1]. This alteration of the immobilization matrix jeopardizing the conformity of the drums regarding current regulations, it is a matter of concern to understand more precisely the root causes of this gel-like product formation and to anticipate if a drum is either going to produce more gel in the future or not.

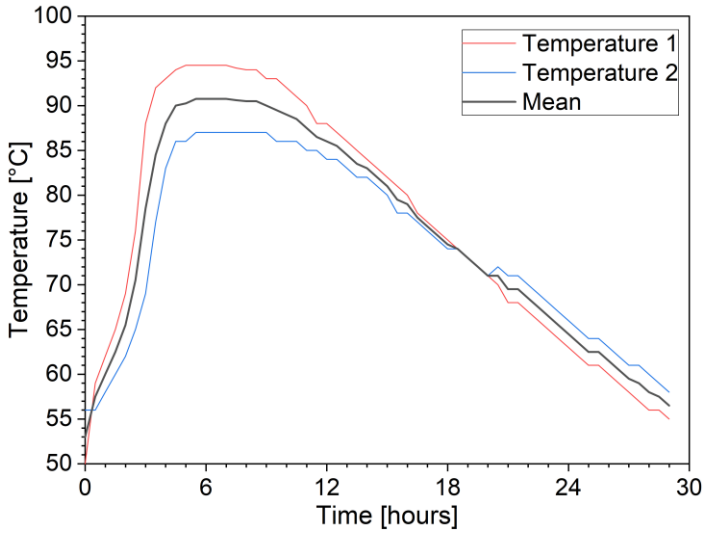

Figure 1.1 Thermal history of the drums incorporating the waste

This work aims at investigating the degradation process of the aggregates submitted to an alkaline solution representative of the pore solution of the cementitious matrix immobilizing the waste.

Flint aggregates (which are representative of those used in the immobilization concrete) and an alkaline solution mimicking the pore solution were poured in stainless steel autoclaves. Since portlandite is the most soluble cement hydrate, calcium hydroxide was added in some of the investigated systems to simulate the cementitious environment. Autoclaves were sealed and heated at 90°C (maximum mean temperature reached by the drums containing the cemented waste) for different durations and were then quenched to stop degradation. The quantity of silica dissolved was assessed by weighing the residual flint aggregates. The degradation state of the remaining aggregates was estimated by investigating the evolution of volumetric mass density, specific surface area and silicate species connectivity along with the degradation duration.

2. MATERIALS AND METHODS

2.1 Analytical techniques

ICP-AES analyses were performed using a Thermo iCAP 6000 spectrometer. Prior to the analysis, samples were diluted in ultrapure water (in order to avoid silicate species precipitation) with a volume ratio of 2000 to analyze silicon content and filtered with 0.45 µm syringe filters. The aerosol was created using argon gas with a flow of 0.5 mL/min.

Volumetric mass densities of the samples were measured using a Micromeritics AccuPyc II 1330 helium gas pycnometer. The analysis chamber had a nominal volume of 1 cm^3 and was calibrated beforehand. Each volumetric mass density value considered hereinafter is the mean value of 20 stable measurements.

Specific surface area values were obtained using a Micromeritics ASAP 2020 surface area system. Prior to the analysis, samples were frozen in liquid nitrogen and freeze-dried at 30 µbar for at least 4 days. Then, they were degassed at 90°C and 3 µbar for 40 hours. Finally, nitrogen sorption isotherms were

obtained within the range $0.05 < P/P^0 < 0.30$, which allowed to apply BET theory and to assess specific surface areas.

^{29}Si solid-state Nuclear Magnetic Resonance spectra have been acquired on a VNMRS400 Varian spectrometer (400MHz / 9,4T). Samples were filled in 7.5 mm zirconia rotors. Spectra were recorded using Magic Angle Spinning (MAS) at 5 kHz. Relaxation time (T1) measurements were performed by using the saturation recovery method. Single-pulse (SP) acquisition was carried out with a π/6 pulse, a recycle delay of 2800 s. ^{1}H – ^{29}Si cross-polarization (CP) measurements were obtained using contact times of 3 ms and a recycle delay of 3 s. Octakis(dimethylsilyloxy)silsesquioxane ($Q_8M_8^H$) has been used as a secondary reference for chemical shifts.

2.2 Experimental program

Two grams of flint aggregate, the granular distribution of which was previously adjusted between 0.16 mm and 0.63 mm by grinding and sieving, were poured in stainless steel autoclaves, pre-heated at 90°C. The airtightness of these autoclaves was checked beforehand, and only those exhibiting less than 2 wt.% leakage after 8 days at 90°C were used thereafter.

One gram of calcium hydroxide was optionally added in the autoclave, allowing investigating the influence of calcium ions on the degradation. This addition aims at simulating the influence of the Portland cementitious matrix by providing a calcium reservoir.

20 mL of alkaline degradation solution were then added in the autoclave in order to cover the solids. Two alkaline degradation solutions, named C1 and C2, were studied in this work. Solution C2 was representative of the waste and contained its main chemical species, whereas C1 was a simplified solution containing only sodium hydroxide and sodium nitrate with the same sodium concentration as C2, and approximately the same pH (see Table 2.1).

After sealing, autoclaves were heated at 90°C for a desired duration. This temperature is representative of the highest temperature reached by the concrete drums incorporating the real waste (see Figure 1.1), after the cementation step. Degradation durations of 4 hours, 15 hours, 1 day and 3 days were chosen in order to monitor the evolution of the system along with the degradation duration and to reach the final balance. Autoclaves were then quenched in an ice-water bath for one hour, in order to stop the degradation reactions and were opened to recover both the liquid and solid phases.

The solid fraction remaining in the autoclave consisted of degraded flint aggregate, residual calcium hydroxide (if some was added in the reactive system) and ions present in the attack solution. The following protocol was applied to recover exclusively degraded flint aggregate [2]: acidic washing (250 mL of 1 mol/L HCl at 700 rpm, 4°C during 1 hour), decantation (2 hours at 4°C) and filtration under vacuum (0.45 µm). The solid was then dried at 40°C for 24 hours before being weighed and characterized by ^{29}Si NMR, helium gas pycnometry and surface area measurement system.

Thus, 20 samples were prepared for this study (5 durations x 2 solutions x $Ca(OH)_2$ addition or not).

A summarizing diagram is given hereinafter in Figure 2.1.

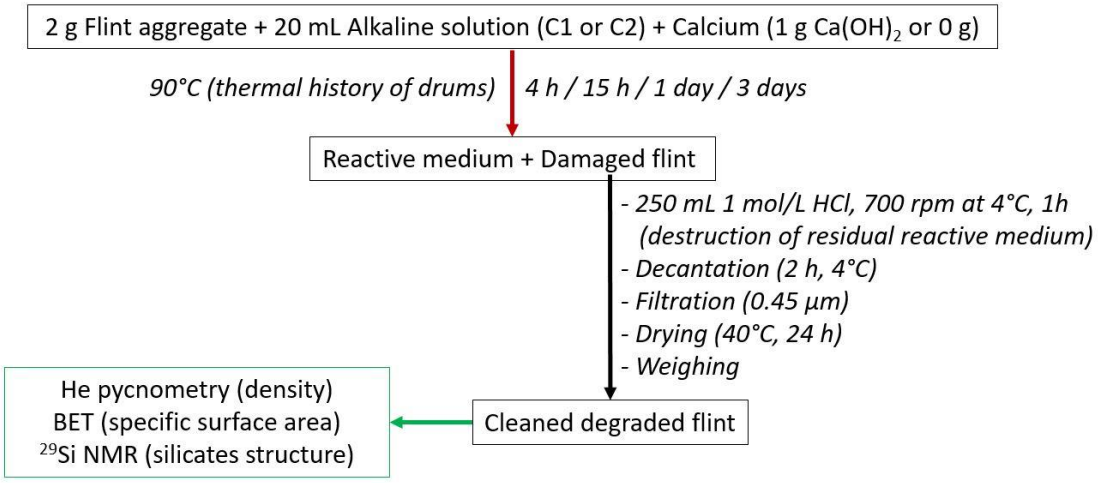

Figure 2.1. Summarizing diagram of the experimental program

2.3 Materials preparation

2.3.1 Flint aggregate

The flint aggregate studied in this work was extracted from a littoral formation of flint pebbles in the North of France. It was representative of the siliceous aggregates used during the 1980's to immobilize the wastes at Doel Nuclear Power Plant. It contained 96 % SiO_2, minor amounts of $CaCO_3$, Al_2O_3, Fe_2O_3 and traces of MgO, Na_2O and K_2O (elemental composition expressed as oxides) as determined by ICP-AES after borate fusion at 950°C and hydrochloric dissolution.

The initial particle-size distribution of the flint aggregate, between 0.063 mm and 16 mm, was adjusted between 0.16 mm and 0.63 mm by grinding and sieving, in order to increase the reactive surface area of the flint aggregate and thus to accelerate the degradation process. Ultra-fine particles were discarded in order to keep exclusively the deleterious fraction regarding alkali-silica reaction.

2.3.2 Attack solutions

The attack solution named C2 was a surrogate containing the main species of the waste. Its composition is detailed in Table 2.1. Powders were added to ultrapure water to reach the desired composition. The heterogeneous solution was then heated at 90°C and stirred at 350 rpm during 46 hours. The remaining undissolved salts were removed by filtration under vacuum at 0.2 µm, in order to avoid silica dissolution coming from both flint aggregate and residual undissolved sodium metasilicate during the degradation. The total theoretical sodium content of this solution was 3734 mmol/kg_{C2}. Its composition was measured by ICP-AES to be 3.1±0.2 mol(Na)/kg_{C2}, 112±6 mmol(Si)/kg_{C2} and 0.027±0.001 mmol(Ca)/kg_{C2}. The lower experimental composition regarding these elements mainly resulted from the reach of a balance between undissolved salts and the solution. In particular, the low experimental dissolved calcium content could result from the low and retrograde solubility of calcium hydroxide in alkaline media [3].

Table 2.1. Theoretical composition of solution C2 (representative of the waste)

Species	Concentration [mmol/kg_{C2}]	Species	Concentration [mmol/kg_{C2}]
Na_2SO_4	127	$NaNO_3$	13
H_3BO_3	1136	NaCl	132
Na_2SiO_3	225	NaOH	2476
$Na_3PO_4 \cdot 12H_2O$	136	$Ca(OH)_2$	279

The second attack solution, named C1, had the same theoretical pH and sodium concentration as C2, but sodium ions were provided exclusively by dissolution of sodium nitrate and sodium hydroxide, leading to a theoretical composition of 1867 mmol(NaOH)/kg_{C1} + 1867 mmol($NaNO_3$)/kg_{C1}. Equilibrium was reached after a few minutes of stirring and led to total dissolution of salts. ICP-AES analysis led to a composition of 3.3±0.2 mol(Na)/kg_{C1}. The slightly lower sodium content than expected could result from water uptake by the salts, which had a hygroscopic behavior.

3. RESULTS AND DISCUSSION

The following notations will be used hereinafter:

- C1: Reactive medium comprising the attack solution C1 and no calcium hydroxide addition;
- C2: Reactive medium comprising the attack solution C2 and no calcium hydroxide addition;
- CaC1: Reactive medium comprising the attack solution C1 and calcium hydroxide addition;
- CaC2: Reactive medium comprising the attack solution C2 and calcium hydroxide addition.

Silicate species are named after Engelhardt nomenclature as Q^n, with n between 0 and 4 being the number of silicon atoms the considered silicon atom is linked with, via oxygen bridges [4]. An illustration diagram is given in Figure 3.1.

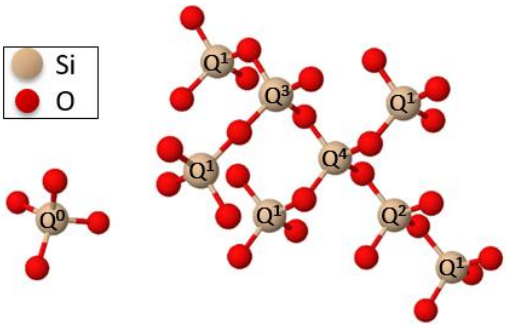

Figure 3.1. Nomenclature of silicate species connectivity – Hydrogen atoms bonded to oxygen atoms (constituting silanol sites) are implicit

3.1 Flint aggregate dissolution

At its natural state, the flint aggregate studied here is predominantly constituted by Q^4 silicon and around 7% Q^3 silicon atoms, which are natural flaws in the flint network [5].

Degradation under the influence of alkaline species (and hydroxyl ions) and temperature rise leads to dissolution of Q^4 silicon atoms by mainly forming Q^0, Q^1 and few Q^2 species, as shown in equations (1) and (2) [6–8].

$$2\ SiO_2\ (\text{i.e. } Q^4) + 2\ NaOH \rightarrow 2\ SiO_{5/2}^{-}\ (\text{i.e. } Q^3) + 2\ Na^+ + H_2O \quad (1)$$

$$SiO_{5/2}^{-}\ (\text{i.e. } Q^3) + Na^+ + NaOH + \frac{1}{2}\ H_2O \rightarrow H_2SiO_4^{2-}(\text{i.e. } Q^0) + 2Na^+ \quad (2)$$

The amount of flint aggregate dissolved during the alkaline degradation is calculated by subtracting the residual mass of flint aggregate after degradation from the mass of flint aggregate initially introduced in the autoclave. Figure 3.2 shows its evolution as a function of time.

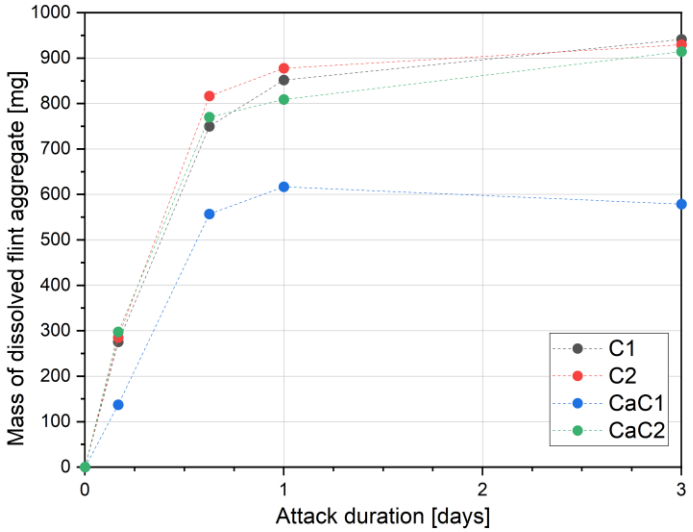

Figure 3.2. Evolution of dissolved flint aggregate along with attack duration. Values are expressed as dissolved mass per gram of flint initially introduced in the autoclave

Both C1 and C2 degradation solutions lead to similar dissolution kinetics without calcium addition. Each solution differing from the other exclusively in terms of other species than sodium, it can be concluded that these minor species do not play a significant role in the dissolution kinetics of flint aggregate, in absence of calcium addition.

Addition of calcium hydroxide to the degradation solution C1 reduces the aggregate dissolution by 25% to 50%. This mitigation can be attributed to the formation of calcium silicate hydrate (C-S-H) or calcium sodium silicate hydrate (C-N-S-H) phases (see equations (3) and (4)) at the surface of the grains.

Indeed, these C-(N)-S-H may behave as a diffusion barrier around the aggregates, which slows down diffusion kinetics of silicate ions outside of the flint aggregate grain [6, 9].

$$H_2SiO_4^{2-} + x\,Ca^{2+} + 2(x-1)OH^- \rightarrow (CaO)x - (SiO_2) - (H_2O)y \quad (3)$$

$$H_2SiO_4^{2-} + x\,Ca^{2+} + 2y\,Na^+ + 2(x+y-1)OH^- \rightarrow (CaO)x - (Na_2O)y - (SiO_2) - (H_2O)z \quad (4)$$

Addition of calcium hydroxide to the degradation solution C2 leads to dissolution kinetics similar to those observed with solutions C1 and C2 without any calcium addition to the reactive medium. This might be attributed to the depletion of calcium to form phosphate and possibly borate minerals of low solubility [10, 11], thus limiting the precipitation of C-(N)-S-H around the aggregate grains.

Whatever the degradation system, the weight of the solid fraction shows limited evolution after 3 days, highlighting the high reactivity of the considered flint aggregate regarding the alkaline waste.

3.2 Flint aggregate characterization

3.2.1 Silicate species connectivity

Relaxation time (T1) has been measured to determine the relaxation delay (D1) required to allow the total relaxation of the observed nuclei (i.e. how quickly equilibrium magnetization is re-established), leading to quantitative single-pulse (SP) analysis.

As shown in Figure 3.3, SP analysis performed on non-degraded flint aggregate leads to a spectrum solely exhibiting one sharp peak centered at -107.2 ppm, attributed to the Q^4 silicon nuclei constituting the flint lattice [4, 6].

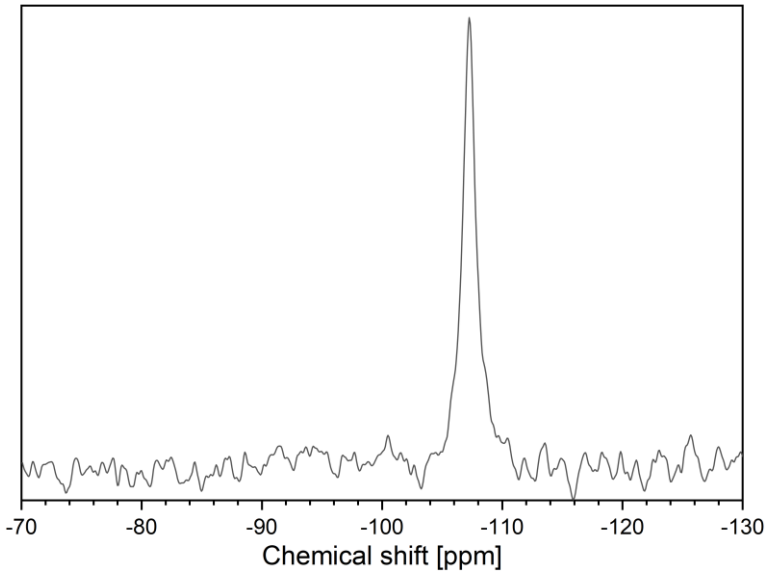

Figure 3.3. Single pulse analysis performed on natural flint aggregate, with D1 = 2800 s

T1 measurement, using saturation recovery pulses sequence, was undertaken on flint aggregate without any degradation and is given in Figure 3.4. As shown in the graph, no plateau is reached even with a saturation delay (τ) increased up to 10 000 s, meaning that some silicon nuclei require a longer T1 to reach total relaxation.

The curve is well fitted using a three components exponential decay function, leading to a longest T1 of 8 289 s. Thus, the D1 value required to restore 99% of initial magnetization is extrapolated to be 41 444 s. This uncommonly high value (values in literature for ^{29}Si NMR analysis are typically in the order of magnitude of tens of seconds) would require total analysis time of about 13 days to carry out 24 transients, which would not even guarantee a satisfying signal/noise ratio for the spectra.

This excessively long T1 value may be imputed to the lack of defects in the flint lattice. Such defects allow indeed an easier and thus faster relaxation of silicon nuclei. This hypothesis is supported by the decrease of T1 value along with degradation duration (T1 = 7234 s for the flint aggregate degraded with solution C1 and no calcium addition during 1 day).

Thus, SP quantitative analysis on the flint aggregate is not practically achievable, hence the limitation of this study to qualitative analysis using cross polarization pulses sequence.

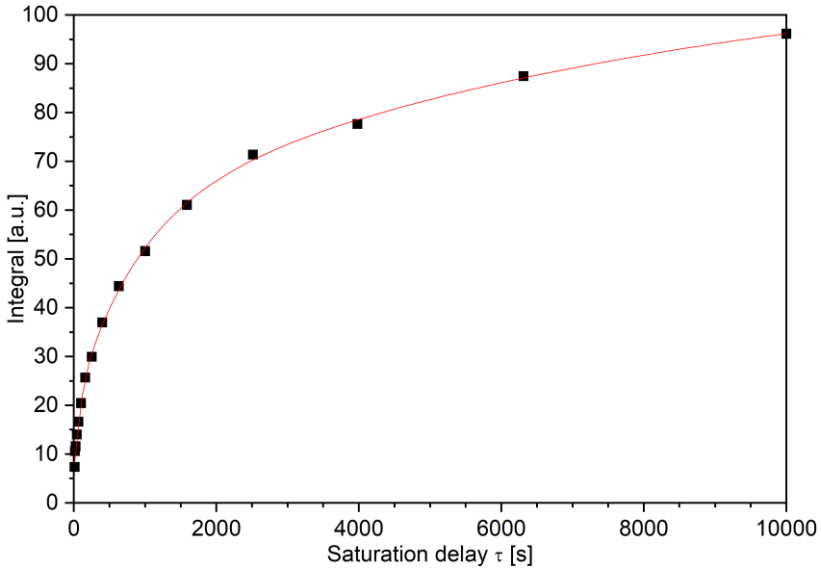

Figure 3.4. T1 measurement of the natural flint aggregate

^{1}H-^{29}Si cross-polarization (CP) technique transfers the magnetization of ^{1}H nuclei to enhance the signal of nearby ^{29}Si nuclei. Thus, the signal of Q^0, Q^1, Q^2 and Q^3 species is increased respectively to the ^{1}H neighboring, which makes it possible to observe them more easily but exclusively leads to qualitative analysis. CP-MAS spectra recorded on flint aggregate degraded up to 3 days are given in Figure 3.5.

CP-MAS spectrum obtained on flint aggregate highlights the natural presence of Q^3 silicon species, which was not noticeable using SP sequence, meaning that the proportion of Q^3 species naturally present in the flint aggregate is around a few percent.

Spectra recorded on flint aggregate submitted to alkaline degradation show the formation of Q^2 and Q^3 species and the elimination of Q^4 species constituting the flint lattice, along with attack duration.

The shift observed for Q^3 species in the degraded samples may arise from a different environment than that of natural flint lattice, i.e. Q^3 species comprised in the neo-formed amorphous phase.

The broad hump appearing within the range -110 ppm to -120 ppm is attributed to the Q^4 silicate species that are not comprised in the natural flint lattice, that is to say Q^4 species in the neo-formed amorphous phase.

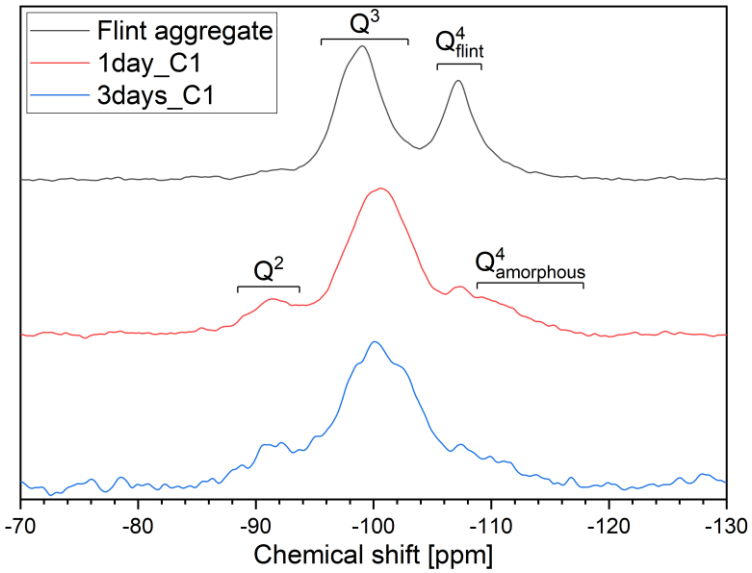

Figure 3.5. Cross-polarization ^{1}H-^{29}Si spectra obtained on flint aggregate, degraded up to 3 days with solution C1 and without calcium addition – Spectra were recorded with 3 ms contact time and D1 = 3 s

3.2.2 Volumetric mass density

The volumetric mass density of the natural flint aggregate was reckoned to be 2.627±0.006 g/cm^3, a slightly lower value than that of crystalline quartz (2.65 g/cm^3 [12]). This value suggests more flaws in the flint lattice than in that of crystalline quartz.

As seen in Figure 3.6, the volumetric mass density of the flint aggregate tends to decrease with ongoing degradation.

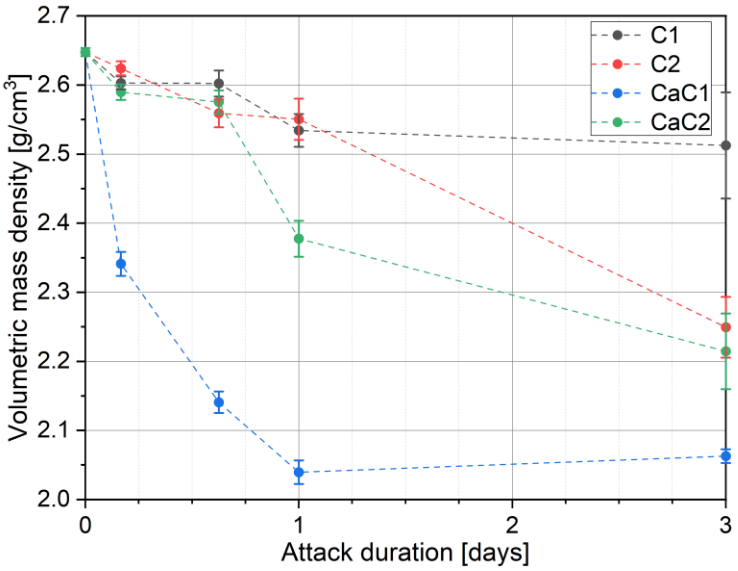

Figure 3.6. Evolution of the flint aggregate volumetric mass density along with attack duration

The attack of the flint aggregate by alkaline ions leads to the formation of Q^3 defects in its network, which results in the opening of this latter. Furthermore, given the basicity of the medium, silanol sites are in an ionized state, electroneutrality is thus insured by cations present in the reactive medium, as shown in equations (5) and (6) [6].

$$SiO_{5/2}^{-} + Na^{+} \rightarrow SiO_{5/2}Na \quad (5)$$

$$2\ SiO_{5/2}^{-} + Ca^{2+} \rightarrow SiO_{5/2}CaSiO_{5/2} \quad (6)$$

These phenomena result in a volume increase of the aggregate, hence a volumetric mass density decrease along with the attack duration.

Solution C2, which has a higher calcium content than C1, produces a higher decrease of aggregate volumetric mass density. Riche noted that neutralization of ionized silanol sites by calcium ions is more prejudicial for volumetric mass density than by alkaline ions [13], which is consistent with our results.

The detrimental effect of calcium is also noticed for CaC1 system, which exhibits the aggregates with the smallest volumetric mass density after 3 days of attack. In system CaC2, where calcium is assumed to precipitate with anions from the waste, the decrease in volumetric mass density is comparable to that of system C2 at 3 days.

3.2.3 Specific surface area

The natural specific surface area of the flint aggregate is found to be 1.0±0.1 m²/g, which agrees well with the value of 0.97±0.05 m²/g found in literature on the same particle-size distribution [5].

As seen in Figure 3.7, the specific surface area of the flint aggregate increases with the attack duration, whatever the degradation system. This rise can be related to the dissolution of silica to form Q^0 entities and to the formation of Q^3 species in the flint network that results in an opening of the aggregate porosity.

Addition of calcium hydroxide to solution C1 increases the specific surface area rise, which can be linked to the limited dissolution of the flint aggregate (see Figure 3.2) and the preferential formation of Q^3 species inside of it [13].

No significant influence of the addition of calcium to the reactive medium is observed for solution C2, whereas calcium addition in solution C1 enhances the increase in specific surface area. This can be attributed to the limited availability of calcium added to solution C2 to precipitate C-(N)-S-H due to competitive reactions with other anions of the waste.

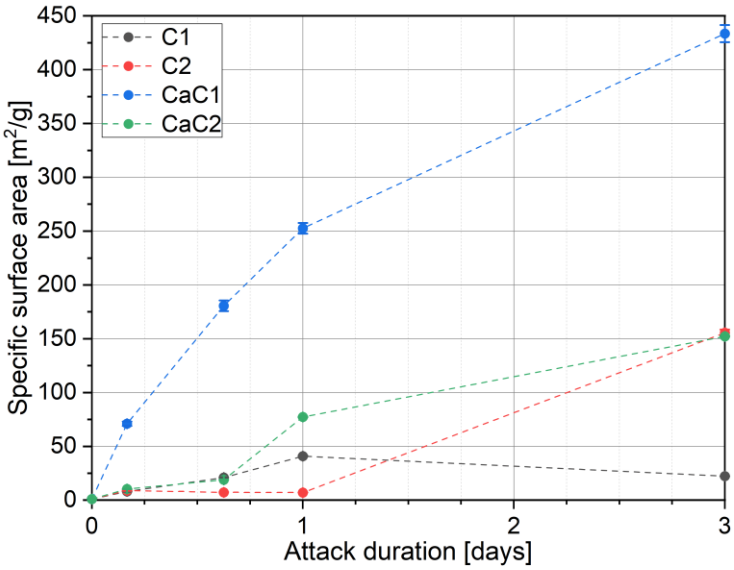

Figure 3.7. Evolution of the flint aggregate specific surface area along with attack duration

4. CONCLUSIONS

^{29}Si NMR experiments outline the complexity of obtaining quantitative information about the evolution of the silicate species connectivity during the alkaline degradation. CP-MAS experiments show the presence of Q^3 defects naturally present in the flint aggregate and the formation of Q^2, Q^3 and Q^4 species, the two latter being in a different environment than the flint lattice, i.e. in the amorphous neo-formed phase.

Calcium addition to the reactive medium limits the flint aggregate dissolution by decreasing the amount of dissolved silicon by 25% to 50 %, if this calcium is available to form C-(N)-S-H phases. The dissolution processes seem to depend solely on the alkaline content of the solution, as no influence of minor species was observed.

Alkaline degradation dissolves silica to form mainly Q^0 entities and creates Q^3 defects in the flint lattice, which opens progressively. The specific surface area of the aggregates is thus increased, as well as their volume, leading to a decrease in their volumetric mass density along with attack duration. When calcium is added to the reactive medium and available for C-(N)-S-H precipitation, a sharper decrease in the volumetric mass density of the grains is observed despite a lower dissolution rate. This confirms the deleterious behavior of calcium ions, leading to higher volume increase of the flint aggregate.

5. ACKNOWLEDGEMENTS

This study was financially supported by ONDRAF, the Belgian National Agency for Radioactive Waste and Enriched Fissile Materials.

The authors would also like to thank “Plateforme d’Analyses et de Caractérisation Balard” (PAC Balard) for technical support concerning the NMR measurements.

6. REFERENCES

[1] ONDRAF/NIRAS (2014) Plan d’actions pour la gestion sûre des fûts présentant du gel. In: ONDRAF. https://www.ondraf.be/plan-dactions-pour-la-gestion-sûre-des-fûts-présentant-du-gel. Accessed 6 Oct 2020

[2] Bulteel D, Garcia-Diaz E, Dégrugilliers P (2010) Influence of lithium hydroxide on alkali–silica reaction. Cem Concr Res 40:526–530. https://doi.org/10.1016/j.cemconres.2009.08.019

[3] Duchesne J, Reardon EJ (1995) Measurement and prediction of portlandite solubility in alkali solutions. Cem Concr Res 25:1043–1053. https://doi.org/10.1016/0008-8846(95)00099-X

[4] Engelhardt LG, Zeigan D, Jancke H, et al (1975) 29Si-NMR-Spektroskopie an Silicatlösungen. II. Zur Abhängigkeit der Struktur der Silicatanionen in wäßrigen Natriumsilicatlösungen vom Na: Si-Verhältnis. Z Für Anorg Allg Chem 418:17–28. https://doi.org/10.1002/zaac.19754180103

[5] Bulteel D, Rafaï N, Degrugilliers P, Garcia-Diaz E (2004) Petrography study on altered flint aggregate by alkali–silica reaction. Mater Charact 53:141–154. https://doi.org/10.1016/j.matchar.2004.08.004

[6] Bulteel D, Garcia-Diaz E, Vernet C, Zanni H (2002) Alkali–silica reaction: A method to quantify the reaction degree. Cem Concr Res 32:1199–1206. https://doi.org/10.1016/S0008-8846(02)00759-7

[7] Garcia-Diaz E, Riche J, Bulteel D, Vernet C (2006) Mechanism of damage for the alkali–silica reaction. Cem Concr Res 36:395–400. https://doi.org/10.1016/j.cemconres.2005.06.003

[8] Iler RK (1955) The Colloid Chemistry of Silica and Silicates, Cornell University Press. Ithaca, New-York

[9] Chatterji S, Thaulow N (2000) Some fundamental aspects of alkali-silica reaction. Quebec, pp 21–30

[10] Elliott JC (1994) Structure and chemistry of the apatites and other calcium orthophosphates. Elsevier, Amsterdam [The Netherlands]: New York

[11] Gode G, Kuka P (1970) Synthesis of calcium borates from aqueous solutions. Zhurnal Neorganicheskoi Khimii 15:1176-

[12] Anthony JW, Bideaux RA, Bladh KW, Nichols MC Handbook of Mineralogy. Mineralogical Society of America, Chantilly, VA 20151-1110

[13] Riche J (2003) La réaction alcali-silice : approche cinétique et mécanisme d’expansion étude du système silex-chaux-potasse à 80°C. Thèse de doctorat, Université des Sciences et Technologies de Lille